for each element in the array — and the outputs of the filters would be summed (see Figure 2). The combination of the spatial diversity of the feed-horn array and the temporal diversity of the filter bank would afford better multipath-suppression performance than is achievable by means of temporal equalization alone.

The seven-element feed array would supplant the single feed horn used in a conventional paraboloidal ground telemetry-receiving antenna. The radio-frequency telemetry signals received by the seven elements of the array would be digitized, converted to complex baseband form, and sent to the FIR filter bank, which would adapt itself in real time to enable reception of telemetry at a low bit error rate, even in the presence of multipath of the type found at many flight test ranges.

Each channel (comprising the signal-processing chain for a receiving feed horn) would contain an $N$-stage FIR filter. The incoming complex baseband signal in the $i$th channel at the $n$th sampling instant is denoted by $y_i(n)$. A filter weight at that instant is denoted generally by $w_{i,j}(n)$, where $i$ is the index number of the channel ($1 \leq i \leq 7$) and $j$ is the index number of the filter stage ($0 \leq j \leq N-1$). The signal-combining operation at the summation (output) point of the FIR filter bank is given by

$$z(n) = \sum_{i=1}^{7} \sum_{j=0}^{N-1} w^*_{i,j}(n) y_i(n-j),$$

where $w_{i,0} \equiv 1$. The weights would be adapted by an algorithm known in the art as the constant-modulus algorithm, embodied in the following equation:

$$w_{i,j}(n+1) = w_{i,j}(n) + \alpha y_i(n-j) z^*(n) [1 - |z(n)|^2],$$

where $\alpha$ is an adaptation rate parameter.

In addition, the combination of the array and the filter bank would make it possible to extract, in real time, pointing information that could be used to identify both the main beam traveling directly from the target aircraft and the beam that reaches the antenna after reflection from the ground: Information on the relative amplitudes and phases of the incoming signals, which information would be indicative of the difference between the antenna pointing direction and the actual directions of the direct and reflected beams, would be contained in the adaptive FIR weights. This information would be fed to a pointing estimator, which would generate instantaneous estimates of the difference between the antenna-pointing and target directions. The time series of these estimates would be sent to a set of Kalman filters, which would perform smoothing and prediction of the time series and extract velocity and acceleration estimates from the time series. The outputs of the Kalman filters would be sent to a unit that would control the pointing of the antenna, enabling robust pointing even in the presence of multipath.

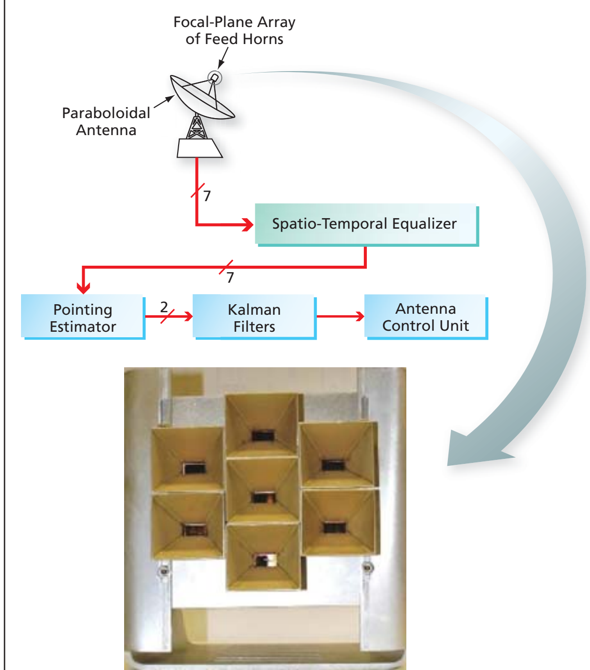


Figure 2. **Seven FIR Filters** would process the seven incoming signals, and the outputs of the filters would be summed.

The performances of several receiving systems with and without multipath and both with and without several conceptual versions of the spatio-temporal equalizer have been demonstrated in computational simulations. It was planned to begin construction of a breadboard version of the spatio-temporal equalizer at or about the time of writing this article.

*This work was done by Ryan Mukai, Dennis Lee, and Victor Vilnrotter of Caltech for NASA's Jet Propulsion Laboratory. Further information is contained in a TSP (see page 1).*

*This invention is owned by NASA, and a patent application has been filed. Inquiries concerning nonexclusive or exclusive license for its commercial development should be addressed to the Patent Counsel, NASA Management Office–JPL. Refer to NPO-43077.*

# High-Speed Ring Bus

## The ring bus is an enhancement of the general high-speed spacecraft bus.

*NASA's Jet Propulsion Laboratory, Pasadena, California*

The high-speed ring bus at the Jet Propulsion Laboratory (JPL) allows for future growth trends in spacecraft seen with future scientific missions. This innovation constitutes an enhancement of the 1393 bus as documented in the Institute of Electrical and Electronics Engineers (IEEE) 1393-1999 standard for a spaceborne fiber-optic data bus. It allows for high-bandwidth and time synchronization of all nodes on the ring. The JPL ring bus allows for interconnection of active units with autonomous operation and increased fault handling at high bandwidths. It minimizes the flight software interface with an intelligent physical layer design that has few states to manage as well as simplified testability. The design will soon be documented in the AS-1393 standard (Serial Hi-Rel Ring Network for Aerospace Applications).

The framework is designed for "Class A" spacecraft operation and provides redundant data paths. It is based on "fault containment regions" and "redundant functional regions (RFR)" and has a method for allocating cables that completely supports the redundancy in spacecraft design, allowing for a complete RFR to fail. This design reduces the mass of the bus by incorporating both the Control Unit and the Data Unit in the same hardware.

The standard uses ATM (asynchronous transfer mode) packets, standardized by ITU-T, ANSI, ETSI, and the ATM Forum. The IEEE-1393 standard uses the UNI form of the packet and provides no protection for the data portion of the cell. The JPL design adds optional formatting to this data portion. This design extends fault protection beyond that of the interconnect. This includes adding protection to the data portion that is contained within the Bus Interface Units (BIUs) and by adding to the signal interface between the Data Host and the JPL 1393 Ring Bus. Data transfer on the ring bus does not involve a master or initiator. Following bus protocol, any BIU may transmit data on the ring whenever it has data received from its host. There is no centralized arbitration or bus granting.

The JPL design provides for autonomous synchronization of the nodes on the ring bus. An address-synchronous latency adjust buffer (LAB) has been designed that cannot get out of synchronization and needs no external input. Also, a priority-driven cable selection behavior has been programmed into each unit on the ring bus. This makes the bus able to connect itself up, according to a maximum redundancy priority system, without the need for computer intervention at startup. Switching around a failed or switched-off unit is also autonomous. The JPL bus provides a map of all the active units for the host computer to read and use for fault management.

With regard to timing, this enhanced bus recognizes coordinated timing on a spacecraft as critical and addresses this with a single source of absolute and relative time, which is broadcast to all units on the bus with synchronization maintained to the tens of nanoseconds. Each BIU consists of up to five programmable triggers, which may be programmed for synchronization of events within the spacecraft of instrument. All JPL-formatted data transmitted on the ring bus are automatically time-stamped.

*This work was done by Terry Wysocky; Edward Kopf, Jr.; Sunant Katanyoutanant; Carl Steiner; and Harry Balian of Caltech for NASA's Jet Propulsion Laboratory. Further information is contained in a TSP (see page 1). NPO-42112*

# Nanoionics-Based Switches for Radio-Frequency Applications

## These switches might supplant semiconductor and MEMS switches in some applications.

*John H. Glenn Research Center, Cleveland, Ohio*

Nanoionics-based devices have shown promise as alternatives to microelectromechanical systems (MEMS) and semiconductor diode devices for switching radio-frequency (RF) signals in diverse systems. Examples of systems that utilize RF switches include phase shifters for electronically steerable phased-array antennas, multiplexers, cellular telephones and other radio transceivers, and other portable electronic devices.

Semiconductor diode switches can operate at low potentials (about 1 to 3 V) and high speeds (switching times of the order of nanoseconds) but are characterized by significant insertion loss, high DC power consumption, low isolation, and generation of third-order harmonics and intermodulation distortion (IMD). MEMS-based switches feature low insertion loss (of the order of 0.2 dB), low DC power consumption (picowatts), high isolation (>30 dB), and low IMD, but contain moving parts, are not highly reliable, and must be operated at high actuation potentials (20 to 60 V) generated and applied by use of complex circuitry. In addition, fabrication of MEMS is complex, involving many processing steps.

Nanoionics-based switches offer the superior RF performance and low power consumption of MEMS switches, without need for the high potentials and complex circuitry necessary for operation of MEMS switches. At the same time, nanoionics-based switches offer the high switching speed of semiconductor devices. Also, like semiconductor devices, nanoionics-based switches can be fabricated relatively inexpensively by use of conventional integrated-circuit fabrication techniques. Moreover, nanoionics-based switches have simple planar structures that can easily be integrated into RF power-distribution circuits.

Nanoionics-based switches exploit the properties of some amorphous materials (in particular, chalcogenide glasses) that can incorporate relatively large amounts of metal and behave as solid electrolytes. The ionic conductivity of such a material can be of the same order of magnitude as the electronic conductivity of a semiconductor. Under appropriate bias con-

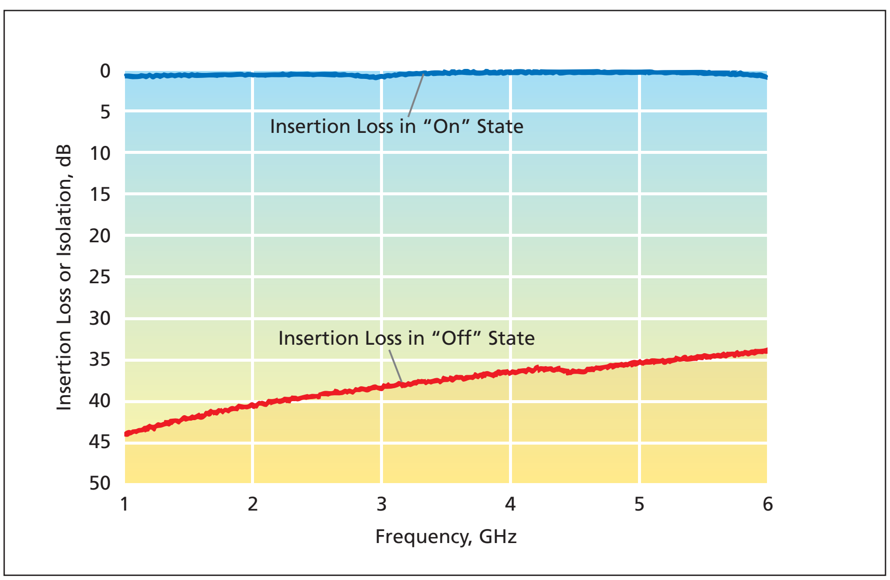


**Insertion Loss and Isolation** — two key switch characteristics — were measured in a test of a nanoionics-based switch over the frequency range of 1 to 6 GHz. The switch characteristics plotted here are comparable and/or superior to those of MEMS and semiconductor switches.